

Technical Notes

TECHNICAL NOTES are short manuscripts describing new developments or important results of a preliminary nature. These Notes cannot exceed 6 manuscript pages and 3 figures; a page of text may be substituted for a figure and vice versa. After informal review by the editors, they may be published within a few months of the date of receipt. Style requirements are the same as for regular contributions (see inside back cover).

J80-~~217~~ 217

Aerothermodynamic Aspects of an Axisymmetric Resonance Tube

C. E. G. Przirembel*

Rutgers University, New Brunswick, N. J. 20015

20007
20009

Introduction

THIS Note presents temperature and pressure measurements for a blunt-edged, axisymmetric Hartmann/Sprenger resonance tube, which was excited by sonic/underexpanded and subsonic air jets. Instantaneous pressure measurements at the endwall and along the tube were made in order to investigate the periodic oscillations characteristic of resonance tubes. Measurements of the wave speed inside the tube were obtained by simultaneously recording the output of two flush mounted pressure transducers installed at a known separation distance. The resulting data may be utilized to construct simple wave and state-plane diagrams.

Experiment

A Hartmann/Sprenger resonance tube consists of a tube, which is closed at one end and mounted with its open end axially aligned with a gas jet. The jet was generated by a simple converging nozzle with a contraction ratio of 2.6 to 1. The nozzle exit diameter was 1.27 cm (0.50 in.). The jet flow conditions were selected by controlling the stagnation pressure P_0 upstream of the contraction. The nozzle exhausted at atmospheric conditions P_a . The ratio of stagnation pressure P_0 to atmospheric pressure P_a was either 1.57 (subsonic) or 2.21 (sonic/underexpanded). The resonance tube had a 1.27 cm (0.50 in.) i.d., a 2.54 cm (1.0 in.) o.d., and a length L of 30.5 cm (12 in.).

Endwall (T_w) and stagnation (T_0) temperatures were measured with copper/constantan thermocouples, and a digital temperature readout device. Time-averaged pressures were measured with standard pressure transducers, while the instantaneous pressure measurements were obtained with flush-mounted Kulite pressure transducers (nominal frequency response: 10,000 Hz) and a storage-type oscilloscope. The oscilloscope traces were recorded photographically.

Results and Discussion

To establish the basic aerothermodynamic characteristics of the current nozzle/resonance tube combination, a series of tests was run for various combinations of trip sizes (b) ($0 \leq b/D \leq 0.21$), jet flow conditions ($1.33 \leq P_0/P_a \leq 2.21$), and separation distances S between the nozzle exit and resonance tube entrance ($0.8 \leq S/D \leq 4.0$). A typical set of curves is shown in Fig. 1. The indicated trip diameter b was

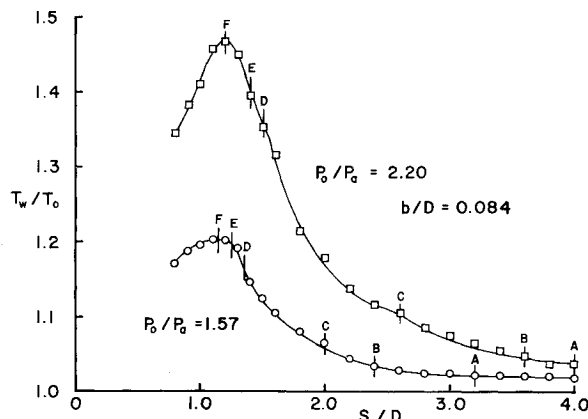


Fig. 1 Endwall temperatures corresponding to Fig. 2.

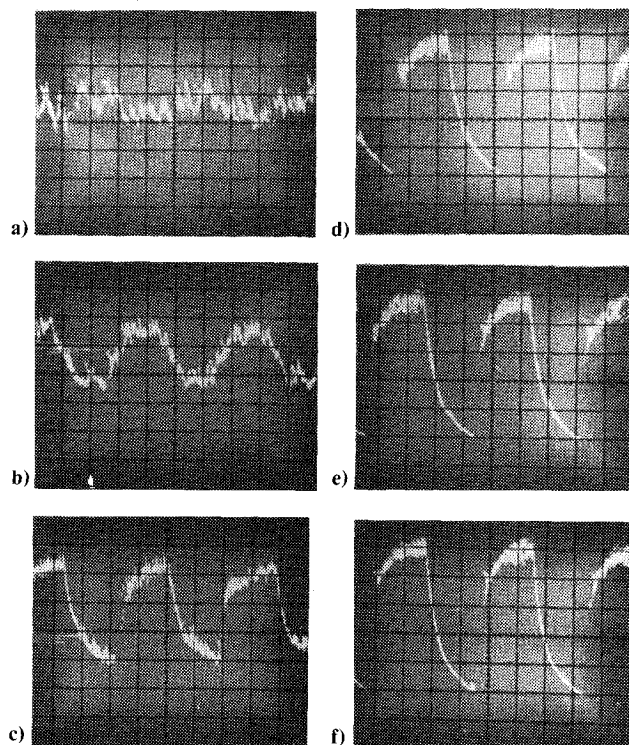


Fig. 2 Endwall transient pressure traces ($P_0/P_a = 2.21$; $b/D = 0.084$; $S/D = 1.1$).

selected from the basic tests as optimizing the maximum endwall temperature. The actual numerical values of the endwall temperatures should be only considered as relative, since they are dependent on the length of a particular test and the cumulative conduction heat losses from the various portions of the resonance tube. Convection losses due to the mixing between the jet and the indigenous gas in the resonance tube are relatively constant. These temperature curves indicate a single, maximum endwall temperature at S/D equal to approximately 1.2. As observed in other experiments, the maximum endwall temperature increased and the position (S/D) for this maximum temperature shifted away from the nozzle exit, as the jet stagnation pressure ratio was increased.

Presented as Paper 78-859 at the 2nd AIAA/ASME Thermophysics and Heat Transfer Conference, Palo Alto, Calif., May 24-26, 1978; submitted Jan. 15, 1979; revision received Feb. 25, 1980. Copyright © American Institute of Aeronautics and Astronautics, Inc., 1978. All rights reserved.

Index categories: Jets, Wakes and Viscid-Inviscid Flow Interactions; Shock Waves and Detonations; Nonsteady Aerodynamics.

*Associate Dean and Professor of Mechanical Engineering. Associate Fellow AIAA.

For the flow and geometric conditions depicted in Fig. 1, transient endwall pressure measurements were obtained. These are shown in Fig. 2. The sensing diaphragm of a Kulite pressure transducer ($P_{\max} = 86 \text{ kPa}$ (50 psi); sensitivity = $0.417 \text{ mV/volt} \times \text{psi}$; input voltage = 6.26 V) was mounted flush with the resonance tube endwall. The transducer signal was monitored on a storage oscilloscope (time scale = 1.0 ms/div. ; voltage scale = 20 mV/div.). The reference pressure was the atmospheric pressure, and the corresponding reference pressure line on the oscilloscope was one division below the X axis.

For large values of S/D , Fig. 2a shows a randomly fluctuating pressure trace, which is consistently above the atmospheric pressure. The initiation of some periodic pressure variations is shown in Fig. 2b, where the trace is essentially sinusoidal in nature. Figures 2c-f show selected pressure traces as the maximum endwall temperature is approached. Starting with trace C, the basic shape of the pressure waveform remains the same. However, the peak-to-peak amplitude continues to increase. The pressure trace is no longer symmetric and sinusoidal, but becomes indicative of the existence of strong compression and expansion waves. An analysis of Fig. 2f showed that the maximum pressure exceeded the jet stagnation pressure by 40%. These high resonance tube pressures support the observations from the flow visualization studies^{1,2} that, during the outflow stage of the cycle, the resonance tube jet appears to penetrate the nozzle jet for a substantial portion of the cycle. Fig. 2f also shows that the lowest pressure in the cycle was one-half of the atmospheric pressure. Hence, there is a substantial underexpansion in the resonance tube. Both of these experimental facts were predicted by Brocher et al.³ in their theoretical analysis of the limit cycle.

The necessity of a trip for resonance conditions in a resonance tube driven by a subsonic jet is clearly demonstrated in Fig. 3. The resonance tube was placed at a separation distance from the nozzle at which the maximum endwall temperature had been reached in the previously-described tests. The jet Mach number was 0.83. The trip diameter ratio was 0.084. Figure 3a indicates the pressure of moving shock waves which characterize strong resonance conditions. In Fig. 3b, the endwall pressure is essentially constant with time and nominally represents the jet stagnation pressure. Similar results have also been reported by Wu et al.^{4,5}

The frequency of oscillation for simple resonance tubes can be calculated from acoustic theory³ as follows:

$$f = C_0 / [4(L + 0.3D)]$$

Using the current resonance tube geometric parameters and the jet temperature to calculate the speed of sound C_0 , a frequency of 278 Hz is predicted. Using Figs. 2 and 3, an experimental frequency of 270-278 Hz was calculated.

In order to analyze the internal flow in more detail, pressure transducers were placed at three different positions along the resonance tube, namely, $x/L = 0.04, 0.40$, and 1.0 . The resulting transient pressure traces are shown in Fig. 4. Considering the pressure trace in Fig. 4b and assuming that the closed end of the resonance tube is to the right, it is possible to specify the following events (note: point 1 designates the lowest pressure in the cycle):

- 1-2: right-traveling shock passes transducers
- 2-3: shock traverses tube, reflects from endwall, and then travels to the left
- 3-4: left-traveling shock wave passes transducer
- 4-5: shock wave moving leftward, reflects from resonance tube inlet in opposite sense, and an expansion wave travels toward the right
- 5-6: expansion wave passes transducer
- 6-7: expansion wave reflects from endwall and travels to the left
- 7-8: expansion wave passes transducer and moves toward resonance tube inlet; a new compression wave forms and moves into resonance tube

Similar analyses can be made of the other two traces. Using these traces, it is possible to calculate the average expansion and compression wave speeds.

In order to obtain still more accurate data on the individual compression/expansion wave speeds, a dual trace oscilloscope was used to record simultaneously two transient pressure traces. For the geometric and flow conditions used in Fig. 4, the data in Table 1 were obtained.

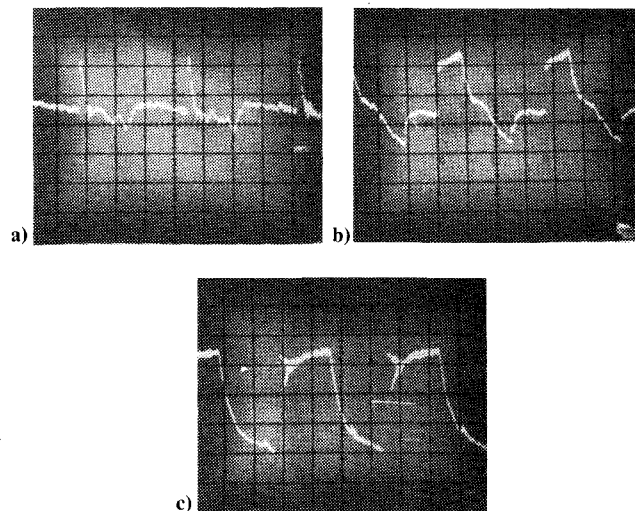


Fig. 3 Endwall transient pressure traces with and without a trip ($P_0/P_a = 1.57$; $b/D = 0.084$; $S/D = 1.1$).

Fig. 4 Transient pressure traces at various axial stations ($P_0/P_a = 1.57$; $b/D = 0.084$, $S/D = 1.1$).

Table 1 Spatially averaged wave speeds

	$0.04 \leq x/L \leq 0.40$		$0.40 \leq x/L \leq 1.0$	
	m/s	fps	m/s	fps
Right-moving compression wave	282	926	356	1167
Left-moving compression wave	299	980	309	1014
Right-moving expansion wave	423	1389	395	1296
Left-moving expansion wave	318	1042	444	1458

The expansion waves travel more rapidly than the compression waves, because the local gas temperature and, hence, the local speed of sound are higher. The higher gas temperatures are the result of the preceding compression processes described in conjunction with Fig. 4.

These results were analyzed by constructing both wave diagrams and state-plane diagrams. Excellent agreement was obtained between the calculated and measured values for various gas dynamic states in a resonance cycle.

Conclusions

The experimental investigation revealed an excellent correlation between the transient pressures and time-averaged temperatures measured at the endwall of a blunt, axisymmetric resonance tube. During various portions of a resonance cycle, transient pressures in the tube exceeded the jet stagnation pressure and, at other times, fell below the ambient pressure level. The reported transient wave pressure amplitudes and the wave speed data can be used to construct wave diagrams and state-plane diagrams. These diagrams are extremely useful in the analysis of the resonance tube phenomenon.

Acknowledgment

This research was carried out with support from the Rutgers Research Council.

References

- ¹Skok, M. W. and Page, R. H., "An Analog Investigation of the Gas Jet Resonance Tube," 5th Cranfield Fluidics Conference, Paper No. D3-37, 1972.
- ²Prizrembel, C. E. G., Page, R. H. and Wolf, D. E., "Visual Studies of Resonance Tube Phenomena," *Proceedings of the International Symposium on Flow Visualization*, Tokyo, Japan, Oct. 1977, pp. 205-210.
- ³Brocher, E., Maresca, C. and Bournay, M. H., "Fluid Dynamics of the Resonance Tube," *Journal of Fluid Mechanics*, Vol. 43, Pt. 2, 1970, pp. 369-384.
- ⁴Wu, J. H. T., Neemeh, R. A. and Ostrowski, P. P., "Resonance Tubes in Under-expanded Jets," *Transactions, Canadian Aeronautics and Space Institute*, Vol. 6, No. 1, 1973, pp. 26-35.
- ⁵Wu, J. H. T., Neemeh, R. A. and Ostrowski, P. P., "Subsonic Jet Driven Resonance Tube," *Transactions, Canadian Aeronautics and Space Institute*, Vol. 8, No. 1, 1975, pp. 29-34.

J80-~~218~~ 218 Steady Oblique Shock-Wave Reflections in Perfect and Imperfect Monatomic and Diatomic Gases

20015

G. Ben-Dor*

*Ben-Gurion University of the Negev,
Beer-Sheva, Israel*

I. Introduction

THE reflection of oblique shock-waves in steady and pseudosteady flows is a nonlinear problem which has been investigated by many researchers for more than three decades. However, only recently, have the oblique shock-wave equations that describe the two and three shock confluences also been solved for imperfect gases.¹⁻³ Utilizing this

solution, the domains and transition boundaries of different types of reflection were established in diatomic² and monatomic³ gases. The analysis was substantiated experimentally. Consequently, it is now possible to predict the type of reflection for a given set of initial conditions.

During the study of the reflection phenomena, it was realized that the domains and transition boundaries of oblique shock-wave reflections in steady flow are not defined completely.

Consequently, it was decided to extend this work to steady flows. This, it is believed will undoubtedly bring added light and order into this complex problem.

II. Analysis

In the following, the different types of oblique shock-wave reflections possible in steady flows, as well as the transition criteria between them, are discussed.

Four types of oblique shock-wave reflections are possible in pseudosteady flows: 1) regular reflections (RR), 2) single-Mach reflection (SMR), 3) complex-Mach reflection (CMR), and 4) double-Mach reflection (DMR). In steady flows, however, only RR and SMR are possible.

Three different criteria for the transition $RR \rightarrow SMR$ exist in the literature. The most quoted criterion is that due to von Neumann,⁴ which is based on the fact that in RR the deflection of the flow by the reflected shock wave R is equal in magnitude, but opposite in sign, to the deflection by the incident shock wave I ; therefore, $\theta_1 + \theta_2 = 0$. This is violated when θ_1 exceeds in magnitude the maximum deflection angle θ_{2m} . This criterion, referred to as the "detachment" criterion (the term detachment comes from steady flows where the oblique shock-wave detaches at this angle), has the following form:

$$\theta_1 + \theta_{2m} = 0 \quad (1)$$

Because of the disagreement between Eq. (1) and steady flow experiments, Henderson and Lozzi⁵ introduced an alternative criterion based on the observation that, in order to maintain the system in mechanical-equilibrium, the $RR \rightarrow SMR$ transition should take place at the point where the R -polar intersects the I -polar (SMR solution) on the P/P_0 -axis (RR solution). Consequently, the mechanical-equilibrium criterion implies that

$$\theta_1 + \theta_2 = \theta_3 = 0 \quad (2)$$

It should be noted that the condition given by Eq. (2) is not always possible. Kawamura and Saito⁶ showed that for incident flow Mach numbers M_0 smaller than a certain "change over" value M_{0c} , the R -polar becomes tangent to the P/P_0 -axis, inside the I -polar, and the situation described by Eq. (2) is unobtainable. For a diatomic gas, $M_{0c} = 2.20 \pm 0.03$, while for a monatomic gas $M_{0c} = 2.46 \pm 0.01$.

Hornung et al.⁷ initiated another criterion for the termination of RR. They argued that in order for a SMR to form, a length scale must be available at the reflection point, i.e., pressure signals must be communicated to the reflection point. Unlike the "mechanical-equilibrium" criterion, the "length scale" criterion applies to the entire range of M_0 . However, while for $M_0 \geq M_{0c}$ it is described by Eq. (2), for $M_0 < M_{0c}$ it reduces to the "sonic" criterion, i.e., $RR \rightarrow SMR$ transition occurs when the flow behind the reflected shock-wave R becomes subsonic. Analytically, the sonic criterion can assume one of the following forms:

$$\theta_1 + \theta_{2s} = 0 \quad \text{or} \quad M_2 = 1 \quad (3)$$

It should be mentioned that in practice the boundary lines obtained from Eqs. (1) and (3) are too close to the resolved experimentally. Note also that the general criterion of Hornung et al.⁷ results in two different transition lines for

Received March 14, 1979; revision received Jan. 16, 1980. Copyright © American Institute of Aeronautics and Astronautics, Inc., 1979. All rights reserved.

Index category: Shock Waves and Detonations.

*Lecturer, Dept. of Mechanical Engineering, Member AIAA.